Crl Binds to Domain 2 of S and Confers a Competitive Advantage on a Natural rpoS Mutant of Salmonella enterica Serovar Typhi

Véronique Monteil, Annie Kolb, Claudine Mayer, Sylviane Hoos, Patrick England, Françoise Norel

Crl binds to domain 2 of σ^S and confers a competitive advantage to a natural *rpoS* mutant of *Salmonella enterica* serovar Typhi

Véronique Monteil[1,2], Annie Kolb[1,2], Claudine Mayer[3,4,5], Sylviane Hoos[4,6], Patrick England[4,6], and Françoise Norel[1,2]

(1) Institut Pasteur, Unité de Génétique moléculaire, Département de Microbiologie F-75015 Paris, France
(2) CNRS, URA2172, F-75015 Paris, France
(3) Institut Pasteur, Unité de Dynamique Structurale des Macromolécules, Département de Biologie Structurale et Chimie F-75015 Paris, France
(4) CNRS, URA 2185, F-75015 Paris, France
(5) Université Paris Diderot, F-75013 Paris, France
(6) Institut Pasteur, Biophysique des macromolécules et de leurs interactions, Département de Biologie Structurale et Chimie, F-75015 Paris, France

Running title: Crl binds to σ^S_2 and rescues a σ^S mutant protein

Key words: *Salmonella*, *crl, rpoS*, sigma factor, RNA polymerase

*** corresponding author**
Institut Pasteur, Unité de Génétique Moléculaire; URA-CNRS 2172; 25 rue du Docteur Roux, 75724 Paris Cedex 15, France. E.mail : francoise.norel@pasteur.fr; Phone : 33 140613122; Fax 33 145688960.

ABSTRACT

The RpoS sigma factor (σ^S) is the master regulator of the bacterial response to a variety of stresses. Mutants in *rpoS* arise in bacterial populations in the absence of stress, probably as a consequence of a subtle balance between self-preservation and nutritional competence. In this study, we characterized one natural *rpoS* mutant of *Salmonella enterica* serovar Typhi (Ty19). We showed that the *rpoS* allele of Ty19 ($rpoS_{Ty19}$) led to the synthesis of a σ^S_{Ty19} protein carrying a single glycine to valine substitution at position 282 in σ^S domain 4, which was much more dependent than the wild-type σ^S protein on activation by Crl, a chaperone-like protein that increases the affinity of σ^S for the RNA polymerase core enzyme (E). We used the bacterial adenylate cyclase two-hybrid system to demonstrate that Crl bound to residues 72 to 167 of σ^S domain 2 and that G282V substitution did not directly affect Crl binding. However, this substitution drastically reduced the ability of σ^S_{Ty19} to bind E in a surface plasmon resonance assay, a defect partially rescued by Crl. The modelled structure of the Eσ^S holoenzyme suggested that substitution G282V could directly disrupt a favourable interaction between σ^S and E. The $rpoS_{Ty19}$ allele conferred a competitive fitness when the bacterial population was wild-type for *crl*, but was outcompeted in Δ*crl* populations. Thus, these results indicate that the competitive advantage of the $rpoS_{Ty19}$ mutant is dependent on Crl and suggest that *crl* plays a role in the appearance of *rpoS* mutants in bacterial populations.

INTRODUCTION

In bacteria, transcription depends on a RNA polymerase (RNAP) consisting of a catalytically active core enzyme (E) with a subunit structure $\alpha_2\beta\beta'\omega$, that associates with any one of several σ factors to form different Eσ holoenzymes. The σ subunit is required for specific promoter binding, and different σ factors direct RNAP to different classes of promoters, thereby modulating the gene expression patterns (17). The holoenzyme containing the σ^{70} subunit is responsible for the transcription of most genes during exponential growth (17). When cells enter stationary phase or undergo specific stress conditions (high osmolarity, low pH or high and low temperatures) during exponential growth, σ^S, which is encoded by the *rpoS* gene, becomes more abundant, associates with E, and directs the transcription of genes essential for the general stress response (17, 18, 21). In *Salmonella* and *Escherichia coli*, the σ^S regulon comprises more than 300 genes contributing to survival during stationary phase, adaptive stress responses, biofilm formation and virulence of *S. enterica* serovar Typhimurium, a wide-host range pathogen and a major cause of human gastroenteritis and food-borne disease (2, 48). However, the precise function of nearly half of the genes in the regulon is unknown.

An intriguing aspect of σ^S is the allelic variation of *rpoS* in *E. coli* and *Salmonella* (9, 13, 36, 38, 50). Because of its role in general stress resistance and its high position in the hierarchy of transcriptional regulators, one might expect σ^S to be conserved in bacteria from different environments. However, *rpoS* mutations accumulate in bacterial populations in the absence of environmental stress (31, 50). Indeed, *rpoS* is not essential in unstressed cells. But, when the culture medium is suboptimal or when bacteria are exposed to additional environmental stresses, the absence of stress resistance resulting from *rpoS* mutations becomes detrimental, and *rpoS* null mutants are outcompeted (31, 40, 50). The selection

pressures on *rpoS* are likely the consequence of a subtle balance between self-preservation and nutritional competence (so-called SPANC balance, 13). σ^{70} is needed for vegetative growth, whereas σ^{S} switches the cell to stress resistance and has a negative effect on the expression of σ^{70}-dependent genes involved in nutrient scavenging and membrane permeability (2, 34, 48). An imbalance between the two sigma factors could reduce the fitness of bacteria in particular situations.

The concentration of σ^{S} is obviously the major but not the only determinant of σ^{S}-dependent gene regulation. Sigma factors compete for a limited amount of E in the cells (16-18, 32). σ^{S} is generally much less abundant than σ^{70} and exhibits the weakest affinity of all σ factors for E *in vitro* (18). The cell uses at least two strategies to ensure the switch between σ^{70} and σ^{S}-associated RNAP and to allow gene expression to be reprogrammed upon entry into stationary phase. Several factors (Rsd, 6S RNA, ppGpp and DksA) indirectly increase σ^{S} competitiveness by decreasing the ability of σ^{70} to bind to E or by inhibiting $E\sigma^{70}$ activity (21). Furthermore, the non-conventional regulatory protein Crl increases the performance of σ^{S} (14, 28, 35, 37, 39, 40, 46). Unlike classical regulators of transcription, Crl binds σ^{S} instead of DNA (3, 12) and the transient interaction of Crl with σ^{S} increases the association rate of σ^{S} to E (12), thereby facilitating RNAP holoenzyme $E\sigma^{S}$ formation (12, 14, 46).

We previously isolated *rpoS* mutants among clinical isolates of *Salmonella enterica* serovar Typhi (36, data not shown). In the present study, we report the characterization of one of these mutants, *S.* Typhi strain Ty19. This mutant initially retained our attention because it produced lower levels of σ^{S} than wild-type strains but was highly resistant to hydrogen peroxide (H_2O_2), a phenotype dependent on σ^{S} activity and used as a tool to screen *rpoS* mutants. We here demonstrate that the low cellular activity of the σ^{S}_{Ty19} mutant protein is partially rescued by Crl and, consistently, that the competitive fitness of the *rpoS*$_{Ty19}$ mutant

is conditioned by the *crl* status of the bacterial population. We also report the identification of a region of σ^S that binds Crl.

MATERIALS AND METHODS

Bacterial strains, plasmids and growth conditions. Strains and plasmids are listed in Table 1. *S.* Typhi clinical strains, including Ty19, were isolated from patients with septicemia and provided by F. Grimont and P. Bouvet from the National Reference Center for *Salmonella* (Institut Pasteur). Bacteriophage P22HT105/1*int* was used to transfer mutations between *Salmonella* strains by transduction (42). Green plates, for screening for P22-infected cells or lysogens, were prepared as described previously (45). Strains were routinely cultured in Luria Bertani medium (LB; 41). Antibiotics were used at the following concentrations: carbenicillin (Cb), 100 μg ml^{-1}; chloramphenicol (Cm), 15 μg ml^{-1} for the chromosomal resistance gene and 30 μg ml^{-1} for the plasmid resistance gene; kanamycin, (Km) 50 μg ml^{-1}; and tetracycline (Tet) 20 μg ml^{-1}.

Oxidative shock survival assay. Cells were grown to stationary phase in LB (optical density at 600 nM (OD_{600}) of 3.5 to 4), washed, resuspended in PBS and mixed with H_2O_2 at a final concentration of 15 mM. Aliquots of bacteria were removed at time intervals, and numbers of colony forming cells were determined on LB plates.

DNA manipulations. Standard molecular biology techniques were used (41). Oligonucleotides were obtained from Sigma-Aldrich (France). DNA sequencing was performed by Beckman Coulter Genomics (France).

Cloning of the *rpoS*$_{Ty19}$ allele. Total DNA from *S*. Typhi Ty19 was cleaved with BglII and the resulting fragments were cloned into the BamHI site of pACYC184. Recombinant plasmids were then transformed into the *E. coli rpoS* mutant strain MC1061K. Transformants harboring plasmids with the 6kb BglII carrying *rpoS*Ty19 fragment (pAC*rpoS*$_{Ty19}$) were selected after colony hybridization with a *rpoS* probe as described previously (22). The presence of *rpoS*$_{TY19}$ on pAC*rpoS*$_{Ty19}$ was checked by DNA sequencing. A 3.5 kb HindIII-ScaI fragment carrying *rpoS*$_{Ty19}$ was subsequently cloned into the HindIII and SmaI sites of pUC19 to yield pUC*rpoS*$_{Ty19}$.

Construction of *S.* Typhi Ty19K and *S.* Typhimurium 2922K*rpoS*$_{Ty19}$. pUCK3Km was used to construct a Δ*rpoS* mutant of *S.* Typhi Ty19. After electroporation in *S.* Typhi Ty19, pUCK3Km appeared to be unstable. Recombination of the *kan* cartridge into the host genome, with simultaneous loss of pUCK3Km, resulted in the isolation of clones that were resistant to kanamycin and sensitive to carbenicillin. The presence of the *rpoS* mutation at the appropriate site in the genome of one clone, designated Ty19K, was confirmed by PCR analyses. The *rpoS* allele in *S*. Typhimurium ATCC14028 was replaced by the *rpoS*$_{Ty19}$ allele using the following strategy (40). pUC*rpoS*$_{TY19}$ contains the *rpoS*$_{Ty19}$ allele of *S.* Typhi strain Ty19 and the downstream genes, including a gene encoding a putative decarboxylase (named STY3047 in *S*. Typhi and STM2922 in *S*. Typhimurium) that is not regulated by *rpoS* (2). In pUC*rpoS*$_{Ty19}$K, a kanamycin resistance (Km) cartridge is located in the SmaI site of STY3047. pUC*rpoS*$_{Ty19}$K was introduced by electroporation into ATCC*rpoS*, where it was unstable. Recombination of the Km cartridge into the host genome with simultaneous loss of pUC*rpoS*$_{Ty19}$K resulted in recombinants that were resistant to kanamycin and sensitive to carbenicillin. A Km^R Cb^S Cm^S recombinant was selected, checked by PCR for the presence of

the STM2922::Km mutation and simultaneous replacement of the Δ*rpoS*::Cm mutation by the *rpoS*$_{Ty19}$ allele. The *rpoS*$_{Ty19}$ and STM2922::Km alleles were then co-transduced to ATCC*rpoS*. Transductants that were Km^R but Cm^S were selected, and transduction of the STM2922 ::Km mutation and simultaneous replacement of the Δ*rpoS* ::Cm mutation by the *rpoS*$_{Ty19}$ allele were confirmed by PCR. One Km^R Cm^S strain, designated 2922K*rpoS*$_{Ty19}$, was also checked by DNA sequencing for the presence of the *rpoS*$_{Ty19}$ allele.

Survival and competition in stationary phase. For survival assays, overnight LB cultures were washed, resuspended in PBS to an OD_{600} of 1.0, diluted in fresh LB medium to about 3000 cells ml^{-1} and incubated at 37°C with shaking. Aliquots of bacteria were removed at timed intervals and numbers of viable cells were determined on LB plates. For competition assays, overnight LB cultures were washed and resuspended in PBS to an OD_{600} of 1.0. Two strains were mixed in equal numbers in fresh LB medium to give a total of about 3000 cells ml^{-1} and the mixture was incubated at 37°C with shaking. Aliquots of bacteria were removed at timed intervals and numbers of viable cells of each strain were determined on LB plates containing the appropriate antibiotics.

Enzymatic assays. β-galactosidase activity was measured as described by Miller (27) and is expressed in Miller units.

BACTH assays. The bacterial adenylate cyclase-based two hybrid (BACTH) assay is dependent upon the functional reconstitution of the *Bordetella pertussis* adenyl cyclase T18 and T25 subdomains by two interacting partners (19). The resulting cAMP binds to and activates the transcription activator CRP, a positive regulator of t□□ *lac* and *mal* operons involved in lactose and maltose catabolism. Derivatives of pUT18 and pKT25, used in the

BACTH assays, were constructed by cloning PCR amplified DNA fragments encoding the protein of interest from *S*. Typhimurium between the PstI and EcoRI sites of pUT18 and the XbaI and KpnI sites of pKT25 as previously described (Table 1, 28). All plasmids were confirmed to be correct by DNA sequencing. The *E. coli cya* strain BTH101 was transformed with derivatives of plasmids pKT25 and pUT18 encoding proteins fused to the T25 and T18 fragments of *Bordetella pertussis* adenyl cyclase. Co-transformants were plated onto MacConkey maltose plates supplemented with carbenicillin, kanamycin and 0.5 mM IPTG to assess the Mal^+ phenotype and on LB plates supplemented with 5-bromo-4-chloro-indolyl-β-D-galactoside (X-Gal, 40 μg ml^{-1}), carbenicillin, kanamycin and 0.5 mM IPTG to assess the Lac^+ phenotype and β-galactosidase activity. Plates were incubated at 30°C for 3 days and colonies were then collected and their β-galactosidase activities were measured as described by Miller (27).

Electrophoresis and immunoblot analysis of proteins. Whole-cell extracts were prepared and SDS-polyacrylamide gel electrophoresis was carried out as described (44). The amount of protein in whole-cell lysates was determined using the DC Protein Assay kit (Bio-Rad). Equal amounts of protein were loaded in each slot. The molecular sizes of the proteins were estimated using molecular size standards (Fermentas, France). Rabbit antibodies against the σ^S protein of *S. enterica* serovar Typhimurium were from Coynault *et al.* (9). Proteins were transferred to Amersham Hybond P membranes (GE Healthcare) and incubated with the polyclonal rabbit antibody serum as previously described (9). Bound antibodies were detected using a secondary anti-rabbit antibody linked to peroxidase and the Amersham ECL plus western blotting detection system kit (GE Healthcare).

***In vitro* transcription.** Single round transcription assays were carried out using pJCD01 plasmid derivatives, which harbour the promoter of interest cloned upstream of the *rrnB* T1 terminator (40). pJCD*poxB* was constructed as follows: the *S.* Typhimurium *poxB* fragment (extending from -97 to +81 relative to the transcription start) was generated by PCR from chromosomal DNA of strain ATCC14028 using primers 5'-GTCAGCGAATTCGGGCGATTTACCACTCGC-3' and 5'-CCAGACCTGCAGACGCCAGCCTGTTCCAGC -3'. The fragment was cleaved by EcoRI and PstI and inserted into the pJCD01 vector cleaved by EcoRI and PstI. *E. coli* core enzyme and *S.* Typhimurium Crl were prepared according respectively to Lederer *et al*., (25) and England *et al*. (12). The DNA encoding $rpoS_{Ty19}$ was amplified using primers HK1 5'-AGGCTCGGATCCATGAGTCAGAATACGCTGAAAGTTCAT-3' and HK2 5'-TTCCGAAAGCTTTTACTCGCGGAACAGCGCTTCGATATT-3' and cloned into the BamHI and HindIII sites of pQE30 to yield pQE30$rpoS_{Ty19}$. The nucleotide sequence of the *rpoS* insert in pQE30$rpoS_{Ty19}$ was checked by DNA sequencing. His_6-σ^S_{WT} and His_6-σ^S_{Ty19} were purified from JM109 carrying plasmids pQE*rpoS* and pQE$rpoS_{Ty19}$ as described in Monteil *et al*. (28), except that the temperature of the cultures were maintained respectively at 28°C and 19°C after 1 mM IPTG addition. For run-off assays, 5 µl of RNA polymerase (σ^S: 300 nM; core: 120 nM) were incubated in buffer A (40 mM Hepes pH 8.0, 10 mM $MgCl_2$, 100 mM K-glutamate, 2 mM DTT supplemented with 500 µg/ml BSA) with 5 µl of buffer with or without Crl (6 µM) for 20 min at 30°C. 5 µl of DNA template were then added at a final concentration of 10 nM and the mixture incubated for 12 min at 30°C. Elongation was started by the addition of a 5 µl mixture containing 1 mM CTP, 1 mM GTP and 1 mM UTP, 100 µM ATP, 1 µCi of [α-^{32}P]-ATP and 600 µg ml^{-1} heparin. After 10 min the reactions were stopped by the addition of formamide containing 10 mM EDTA, xylene cyanol, bromophenol blue and 1 % sodium dodecyl sulfate (SDS). After heating to 90°C, samples were subjected to

electrophoresis on a 7% polyacrylamide sequencing gel and the transcripts were quantified using a PhosphorImager (Molecular Dynamics).

Molecular modelling. The structure of σ^S was modelled using the σ^{70} of the *T. thermophilus* holoenzyme structure (chain F, PDB code 1IW7, 47) as a template, with the CPHmodels 3.0 Server (30) and was manually corrected based on sequence alignement. The structure was energy minimized in 100 steps with a dielectric constant of 1, using the program CNS (4). The model spans residues 53 to 314. The modelled σ^S was docked onto E by superimposing the σ^S coordinates with those of σ^{70} from the *T. thermophilus* holoenzyme structure (1IW7). The figures were generated using PyMOL (10).

Surface plasmon resonance. Experiments were performed as previously described (12), using a Biacore 2000 instrument (GE Healthcare) equilibrated at 25°C in buffer A supplemented with 0.034% Tween 20. The monoclonal antibody 4RA2 (Neoclone), directed against RNAP, was covalently immobilized on two flowcells of a CM5 sensorchip (GE Healthcare). 2000-2500 resonance units (RU, ≈ pg/mm^2) were captured on one of the surfaces, while the other was left unliganded and used as a reference. σ^S_{WT} or σ^S_{Ty19} (20 nM to 2.5 µM), alone or pre-equilibrated with Crl (5 µM), were then injected over the two surfaces for 3 min at 20 µl/min, and the dissociation was then followed for 5 min. All the association and dissociation profiles were double-referenced using the Scrubber 2.0 software (BioLogic software) (i.e. both the signals from the reference surface, and from blank injections of Crl or running buffer were subtracted).

RESULTS

Characterization of *rpoS*$_{Ty19}$, a natural *rpoS* mutant allele of *S.* Typhi

During a search for *rpoS* mutants in clinical isolates of *Salmonella* (36 and data not shown), our attention was drawn by *S.* Typhi strain Ty19, a strain isolated from human blood. *S.* Typhi Ty19 produced a low amount of σ^S (Figure 1, lane 2), compared to wild-type isolates of *S.* Typhi (Figure 1 lane 1, and 36). Surprisingly, Ty19 was resistant to hydrogen peroxide (H_2O_2) in stationary phase (Figure 2A, lanes 1 and 3), a phenotype dependent on σ^S (Figure 2A lanes 1 and 5). The sequence of the promoter and leader regions of the *rpoS* gene in Ty19 (*rpoS*$_{Ty19}$) was wild-type but the open-reading frame contained a G/T mutation at position 845, which resulted in a glycine to valine amino-acid substitution at residue 282 (G282V) in the σ^S_{Ty19} protein.

The chaperone-like protein Crl increases the performance of σ^S but its impact on the H_2O_2 resistance level of *S.* Typhimurium in stationary phase is hardly detectable in standard growth conditions (37, 40). Most interestingly, a *crl* mutation affected the ability of *S.* Typhi Ty19 to resist to H_2O_2 (Figure 2A, lanes 3-4), whereas, as expected, no significant effect of the *crl* mutation was detected on the H_2O_2 resistance level of strain 5959 (Figure 2A, lanes 1-2), a *S.* Typhi strain wild-type for *rpoS* (36). At low cell density, the effect of the *crl* mutation on the H_2O_2 resistance level of Ty19 was drastic and not highly different from that of the *rpoS* deletion (Figure 2B). These results suggested that the σ^S activity in Ty19 was more dependent on Crl activation than in strain 5959.

The activity of σ^S_{Ty19} is highly dependent on Crl

To characterize the *rpoS*$_{Ty19}$ allele in an otherwise isogenic background, the *rpoS* gene from *S.* Typhimurium ATCC14028 was replaced by the *rpoS*$_{Ty19}$ allele yielding strain

2922K*rpoS*$_{Ty19}$. As previously observed in *S.* Typhi, σ^{S}_{Ty19} was detected in lower amounts than the wild-type σ^{S} protein (Figure 1 lanes 4 and 7). Interestingly, levels of H_2O_2 resistance were more dependent on Crl in the *rpoS*$_{Ty19}$ mutant than in the wild-type strain (Figure 2C). Consistent with this finding, the expression level of a *lacZ* gene fusion in *katE*, a σ^{S}-dependent gene encoding a catalase required for the H_2O_2 resistance of *Salmonella* in stationary phase (37), was affected by the *crl* mutation in the *rpoS*$_{Ty19}$ mutant but not in the wild-type strain (Figure 2D lanes 4-5 and 1-3). σ^{S}_{Ty19} production levels were not lowered in the absence of Crl (Figure 1, lanes 7-8). These results suggested that the activity of σ^{S}_{Ty19} was highly dependent on Crl activation. At low cell density, the *rpoS*$_{Ty19}$ mutant was slightly less resistant to H_2O_2 than the wild-type strain (Figure 2C) and expressed the *katE-lacZ* fusion to slightly lower levels (Figure 2D).

In agreement with the *in vivo* data, *in vitro* transcription experiments using three different σ^{S}-dependent promoters, *katE, katN* and *poxB*, demonstrated that the activity of the σ^{S}_{Ty19} protein was lower, and much more dependent on Crl activation, than that of the wild-type σ^{S} protein (Figure 3A). In these assays, addition of Crl rescued σ^{S}_{Ty19} activity to a level similar to that obtained using the wild-type σ^{S} protein in the absence of Crl (Figure 3A). In conclusion, the G282V substitution in σ^{S}_{Ty19} both decreased the activity of σ^{S} and increased its dependency to Crl activation.

σ^{S}_{Ty19} depends on Crl for binding to RNAP core

In vitro transcription assays showed that the activity of σ^{S}_{Ty19} is impaired, and that this defect is rescued by Crl (Figure 3A). Because Crl favors σ^{S} binding to the RNAP core enzyme E, one possibility to explain this finding is that Crl compensates a low E-binding propensity of σ^{S}_{Ty19}.

To study the interaction between σ^{S}_{Ty19} and E, we used a surface plasmon resonance (SPR) assay that we had previously set-up (12). A monoclonal antibody specific for the C terminus of the RNAP α subunit (α-CTD; which plays no role in the association of σ with E) was covalently immobilized to the dextran surface of a sensor chip and used to capture E noncovalently.

We observed that, in the absence of Crl, no binding of σ^{S}_{Ty19} (up to 2.5 μM) to E could be detected (Figure 3B). On the contrary, in the presence of Crl, the ability of σ^{S}_{Ty19} to bind to E was restored to a level similar to that observed with the wild-type σ^{S} protein in the absence of Crl (Figure 3B), in agreement with the *in vitro* transcription data (Figure 3A). Altogether, these results showed that σ^{S}_{Ty19} is impaired for E binding and that this defect is alleviated by Crl.

G282 is located in a flexible loop in region 4 of σ^{S}

Sequence alignments of σ^{70} family members, to which σ^{S} belongs, have revealed that they are constituted of four conserved regions (regions 1-4, Figure 4B) (26, 29, 33). Among these, region 2 (subregions 2.1 to 2.4) and region 4 (subregions 4.1 and 4.2) contain DNA-binding domains that mediate recognition of the conserved –10 and –35 elements of σ^{70}-dependent promoters, respectively. The linear division of σ^{70} factors into functionally distinct regions has been largely confirmed by structural data, which revealed that primary sigma factors have four flexibly linked domains, $\sigma_{1.1}$, σ_2, σ_3 and σ_4, containing regions 1.1, 1.2-2.4, 3.0-3.1, and 4.1- 4.2, respectively (6, 7, 26, 29, 33, Figure 4AB). The $\sigma_{1.1}$ region is unstructured in all available crystal structures. Additionally, the linker between σ_3 and σ_4 corresponds to region 3.2 (Figure 4AB). Regions 2 and 4 are not only involved in DNA binding but also contain critical determinants for binding the β' and β subunits of the RNAP,

respectively (1, 29) (Figure 5A). The G282V substitution is located in region 4 of σ^{S}_{Ty19} (Figure 4B).

In the $E\sigma^{70}$ holoenzyme, the σ subunit stretches across the upstream face of the enzyme, making extensive contacts with subunits β and β' of the RNAP and with its DNA recognition elements positioned to contact the promoter (29). A flexible flap domain of subunit β of the RNAP (β-flap), interacts with region 4 of σ^{70}, involving mainly residues belonging to the flexible loop between helix H2 and helix H3 of σ_4, positioning region 4.2 to interact with the –35 promoter element, αC-terminal domain and activators (11) (Figure 5). This interaction depends on a hydrophobic patch on one face of the short helix stretch located at the tip of the flap domain, called the β-flap-tip helix (15). The contact between the β-flap-tip helix hydrophobic patch and the σ hydrophobic region is essential for the stable interaction of the β-flap-tip helix with the H2-H3 loop. The σ_4 domain (region 4.1-4.2) is C-shaped, with a concave pocket coated with hydrophobic residues of region 4.1. In the holoenzyme, the β-flap-tip helix fits into this concave pocket (Figure 5).

In the structure of the modelled σ^{S}, based on the structure of *T. thermophilus* σ^{70} (47), the G282 residue is located at the top of the H2-H3 flexible loop (residues L280-E289, Figure 4A). When docked onto E, this loop lies in a cleft formed by the β-flap on one side and the β' zinc finger on the other side (Figure 5). Interestingly, both the β-flap and the β' zinc finger region sequences are highly conserved between *Thermus thermophilus* and *Salmonella enterica.* In contrast, the residues corresponding to G282 in σ^{70} are either an aspartate or a methionine, whose side chains easily accommodate into the E cleft as observed in the *T. thermophilus* $E\sigma^{70}$ holoenzyme (47). Substitution G282V could directly disrupt the interaction between σ^{S} and E through two different mechanisms. First, G282V could modify the conformation of the H2-H3 loop by increasing its rigidity and thus reducing its capacity to

interact with the β-flap. Second, the interaction of the loop with the β-flap could be sterically destabilized because of the presence of the valine side-chain.

Crl binds to domain 2 of σ^S

So far, the σ^S domain involved in Crl binding remained unknown. To understand better the effect of the G282V substitution on the interaction between Crl and σ^S, the bacterial two-hybrid system (BACTH system, 19) was used. In this system, the T25-σ^S and Crl-T18 hybrid proteins were shown to interact, yielding levels of β-galactosidase activity higher than those detected in negative controls (Figure 4B and 28). We previously showed that the first 71 residues of σ^S were not required for Crl binding since the T25-$\sigma^S_{72\text{-}330}$ and Crl-T18 chimeras interacted efficiently (28 and Figure 4B). The level of β-galactosidase activity detected with T25-$\sigma^S_{72\text{-}330}$ was actually higher than with T25-σ^S, which might be due to the higher expression of T25-$\sigma^S_{72\text{-}330}$ compared with T25-σ^S, as detected by immunoblotting with a polyclonal σ^S antibody (28, Figure 4B and data not shown). For the T25-σ^S_{Ty19} chimera, levels of β-galactosidase activity were also higher than for the T25-σ^S chimera (Figure 4B), but in this case the amount of T25-σ^S_{Ty19} detected by the σ^S antibody was lower than that of T25-σ^S (data not shown).

To determine whether the C-terminal domain of σ^S interacts with Crl, truncated variants of the T25-σ^S chimera were assessed in the BACTH. The T25-$\sigma^S_{90\text{-}330}$, T25-$\sigma^S_{169\text{-}330}$, and T25-$\sigma^S_{238\text{-}330}$ chimeras, did not yield significant β-galactosidase activity (Figure 4B) although the protein amounts were similar to that of the T25-$\sigma^S_{72\text{-}330}$ chimera, as assessed by immunodetection with the σ^S antibody (data not shown). In contrast, the five chimeras T25-$\sigma^S_{1\text{-}254}$, T25-$\sigma^S_{72\text{-}254}$, T25-$\sigma^S_{1\text{-}167}$, T25-$\sigma^S_{56\text{-}167}$, and T25-$\sigma^S_{72\text{-}167}$ yielded levels of β-galactosidase activity in the BACTH that were higher than that detected with the T25-σ^S

chimera, showing that they were able to interact with the Crl-T18 protein (Figure 4B). These chimeras were barely or not detectable by the σ^S polyclonal antibody (data not shown), suggesting either that their amounts were low or that these chimeras did not react efficiently with the σ^S antibody. Altogether, these results demonstrated that amino acids 72 to 167 in σ^S are sufficient for interaction with Crl. Interestingly, the G282V substitution in T25-$\sigma^S_{90\text{-}330}$ and T25-$\sigma^S_{238\text{-}330}$ did not allow them to interact with Crl-T18 (Figure 4B). Thus this substitution likely favors the interaction of T25-σ^S_{Ty19} with Crl-T18 indirectly, through conformational changes of T25-σ^S_{Ty19}.

rpoS$_{Ty19}$ confers a competitive fitness to _Salmonella_, conditional to the _crl_ status of the bacterial population.

One likely hypothesis to explain the appearance of the _rpoS_$_{Ty19}$ allele in natural isolates of *S.* Typhi is that this mutant allele confers a competitive fitness. We previously set up a survival assay with mixed populations of *Salmonella* in which the Δ*crl* mutation increased the competitive fitness of *Salmonella* in stationary phase (40). We used this assay to assess the competitive fitness of strains carrying the _rpoS_$_{Ty19}$ allele.

Two strains of *Salmonella* were mixed in equal cell numbers in LB liquid medium, and the numbers of each were monitored for several days (Figure 6B). The _rpoS_$_{Ty19}$ mutant showed a competitive advantage during stationary phase over wild-type strain ATCC14028 (Figure 6B panel c). Two days after inoculation of the medium, _rpoS_$_{Ty19}$ mutant cells represented more than 80% of the total population. However, the gain of fitness afforded by the _rpoS_$_{Ty19}$ allele was lost in a population carrying a deletion of the *crl* gene. Indeed, in Δ*crl* context, strains carrying the _rpoS_$_{Ty19}$ allele were outcompeted by strains carrying a wild-type *rpoS* allele (Figure 6B, panel d). In a similar way, the Δ*rpoS* mutant was outcompeted by the wild-type strain (40, Figure 6B) suggesting that the gain of fitness afforded by the _rpoS_$_{Ty19}$

mutation is conditional upon the presence of *crl*. Vice-versa, the Δ*crl* mutant also showed a competitive advantage over the wild-type strain (Figure 6B panel e) but this gain of fitness was lost in populations carrying the $rpoS_{Ty19}$ allele (Figure 6B, panels f and h). In control experiments, wild-type strain ATCC14028 showed similar fitness as wild-type strain 2922K (Figure 6B panel a) and the Km or Cm resistance cartridges, harbored by some of the strains, had no effect (Figure 6B panels a and g and 40). Finally, we observed no significant differences when comparing the ability of wild-type and mutant strains to survive in monocultures under the same conditions (Figure 6A).

DISCUSSION

In this study, we show that the natural *rpoS*$_{Ty19}$ mutant allele of *S*. Typhi Ty19 leads to the synthesis of a σ^{S}_{Ty19} protein with a very low E-binding propensity due to a G282V substitution in the σ_4 domain. All σ_4 domains of the σ^{70} family have a common structural fold but present different electrostatic surface potentials (24); σ^{S} domain 4 is more acidic than its σ^{70} counterpart and has been shown to bind with a higher apparent affinity to the β-flap of RNAP in a bacterial two-hybrid assay (23). Since the overall affinity of σ^{S} for E is lower than that of σ^{70} (18), it is possible that the interaction between σ^{S}_4 and the β-flap plays a crucial role in the stability of Eσ^{S} and that any substitution (such as G282V) weakening this interaction would thus impede the formation of the holoenzyme. The findings that Crl can bind and rescue σ^{S}_{Ty19} efficiently (Figures 3 and 4B), indicate that residue G282 is not in itself crucial for the interaction with E, but rather that σ^{S}_{Ty19} is blocked in a conformation incompatible for E binding.

Production of σ^{S} is tightly regulated through a combination of regulatory mechanisms operating at different levels (reviewed in 21). Rapid degradation of σ^{S} in growing cells depends on the ClpXP protease and the RssB protein which is required to deliver σ^{S} to ClpXP. In stationary phase, there is a reduction of σ^{S} proteolysis and accumulation of σ^{S} (21). The steady state levels of σ^{S}_{Ty19} in stationary phase were lower than those of σ^{S} (Figure 1) but the half-lifes of the proteins were not significantly different (data not shown). However, in the exponential phase, the amounts of σ^{S}_{Ty19} were below the level of detection (data not shown) and we cannot exclude a negative effect of the G282V substitution on the stability of the protein. Alternatively, the mutation in *rpoS*$_{Ty19}$ may affect the efficiency of translation and/or the stability of the mRNA. Clearly, additional experiments are required to address this issue.

Crl has a dual role in σ^S proteolysis (35, 46). On one side, Crl stimulates the σ^S-dependent transcription of *rssB*, and thereby increases σ^S degradation (46). On the other side, σ^S is protected from degradation within the holoenzyme (51) and the function of Crl in favour of $E\sigma^S$ formation results in increased σ^S stability (46). This positive effect of Crl on σ^S stability, which would result in higher levels of σ^S in the presence of Crl, is masked by the effet of Crl on *rssB* expression and cellular amounts of σ^S are higher in the absence of Crl (35, 46, 39, Figure 1 lanes 4-5). Surprisingly, no effect of the *crl* mutation was detected on the cellular amounts of σ^S_{Ty19} (Figure 1, lanes 7-8). It is likely that, in the *rpoS*$_{Ty19}$ mutant, the inverse effects of Crl on σ^S_{Ty19} stability, through E-σ^S_{Ty19} formation and induction of the σ^S_{Ty19}-dependent *rssB* transcription, fully compensate each other.

Negative control of gene expression by σ^S appears to be as significant as positive control (2, 34) and to result in a growth advantage of *rpoS* mutants and their selection in bacterial populations (13, 31, 40, 50). Indirect mechanisms, such as activation of repressors or sigma factor competition for E-binding, are presumably involved in the negative regulation by σ^S. σ^S is needed for competitive fitness in stationary phase (40, 50, Figure 6B) but the lower than wild-type functionality of σ^S in the *rpoS*$_{Ty19}$ mutant (Figure 2CD, Figure 3 and data not shown) resulted in gain of competitive fitness (Figure 6B). This is probably because, in the conditions used, there is a good compromise in this strain between reduction of expression of σ^S -dependent genes required for survival and stress resistance on the one hand, and increased expression of σ^{70}-dependent genes required for persistence and/or growth on the other hand. Interestingly, the gain of fitness afforded by the *rpoS*$_{Ty19}$ mutation was conditional upon the presence of *crl* (Figure 6B), suggesting that, under these conditions, the level of σ^S_{Ty19} activity in the absence of Crl is below the threshold required for *Salmonella* fitness. This flexibility of σ^S_{Ty19} activity might allow bacteria to adjust the level of σ^S activity in the *rpoS*$_{Ty19}$ mutant to

varying environments through regulation of *crl* expression or secondary mutations in *crl*. In this regard, the *rpoS*$_{Ty19}$ mutant provides a genetic tool that may facilitate the identification of *crl* mutants and/or mutants affected in the regulation of *crl* expression. These results suggest a role for *crl* in the appearance of *rpoS* mutants and raise the possibility that a number of *rpoS* mutations in bacterial populations have escaped our attention due to the capacity of Crl to rescue the activity of the corresponding σ^S mutant proteins.

There is no 3D-structure available for full-length free σ but several lines of evidence suggest that free σ adopts a compact (closed) conformation, incompatible with promoter recognition and different from its open structure in Eσ complexes (7, 43). Indeed, binding to E induces large movements of the σ domains (5, 7, 29), switching σ into an active conformation in which the DNA binding determinants in σ_2 and σ_4 are exposed (29). The regulation of many key biological processes in bacteria is fine-tuned by the interplay between σ factors and their cognate anti-σ factors (7). Proteins that bind σ factors typically reduce their efficiency by restricting their access to E. In contrast, the transient interaction of Crl with σ^S increases the association rate of σ^S to E (12), thereby facilitating RNA polymerase holoenzyme Eσ^S formation (12, 14, 46). One attractive model is that Crl acts as a unique, chaperone-like protein, favouring an open conformation of σ^S with a high E-binding propensity.

Among the structurally characterized anti-σ factors, all but the AsiA interact with two or more structural domains of σ simultaneously (7, 49). In each case, the complex that is formed precludes a functional interaction between σ and E. In contrast, AsiA, which functions in the context of Eσ^{70}, interacts only with domain 4 of σ^{70}, selectively inhibiting the utilization of –10/-35 promoters. Our results reveal that Crl interacts with domain 2 of σ^S (Figure 4B). We cannot rule out the possibility that Crl contacts transiently and/or weakly an

additional domain of σ^S, besides the σ^S_2 domain, thus making this association difficult to detect in the BACTH assay. However, the affinity of Crl for σ^S is low (around 2 μM) and the Crl-σ^S complex has a short half-life (less than 3sec). These findings suggest that Crl does not form extended interfaces with σ^S and are consistent with the binding of Crl to a single domain of σ^S. Experiments are in progress to determine which amino acids of the σ^S_2 residues 72 to 167 are directly involved in Crl binding and to investigate the mechanism of action of Crl in greater detail by structural and biophysical approaches**.**

Acknowledgments:

We are grateful to Anthony Pugsley for reading of the manuscript and for his support.

REFERENCES

1. **Arthur, T.M., and R.R. Burgess.** 1998. Localization of a sigma70 binding site on the N terminus of the *Escherichia coli* RNA polymerase β' subunit. J Biol Chem. **273**:31381-7.

2. **Bang, I.-S., J. G. Frye, M. McClelland, J. Velayudhan, and F.C. Fang**. 2005. Alternative sigma factor interactions in *Salmonella*: σ^E and σ^H promote antioxidant defences by enhancing σ^S levels. Mol. Microbiol. **56**: 811-823.

3. **Bougdour, A., C. Lelong, and J. Geiselmann.** 2004. Crl, a low temperature-induced protein in *Escherichia coli* that binds directly to the stationary phase sigma subunit of RNA polymerase. J. Biol. Chem. **279:**19540-50.

4. **Brünger, A.T., P.D. Adams, G. M. Clore, W. L. DeLano, P. Gros, R. W. Grosse-Kunstleve, J. S. Jiang , J. Kuszewski, M. Nilges, N. S. Pannu, R. J. Read, L. M. Rice, T. Simonson, and G. L. Warren**. 1998.Crystallography & NMR system: A new software suite for macromolecular structure determination. Acta Crystallogr. D. Biol. Crystallogr. **54**:905-21.

5. **Callaci, S., E. Heyduk, and T. Heyduk**. 1999. Core RNA polymerase from *E. coli* induces a major change in the domain arrangement of the sigma 70 subunit. Mol. Cell. **3**: 229-138.

6. **Campbell, E. A., O. Muzzin, M. Chlenov, J. L. Sun, C. A. Olson, O. Weinman, M. L. Trester-Zedlitz, and S. A. Darst.** 2002. Structure of the bacterial RNA polymerase promoter specificity σ subunit. Mol. Cell **9**: 527-539.

7. **Campbell, E. A., L. F. Westblade, and S. A. Darst**. 2008. Regulation of bacterial RNA polymerase σ factor activity: a structural perspective. Current Opin. Microbiol. **11**: 1-7.

8. **Chang, A. C., and S. N. Cohen.** 1978. Construction and characterization of amplifiable multicopy DNA cloning vehicles derived from the P15A cryptic miniplasmid. *J. Bacteriol*. **134:** 1141-56.

9. **Coynault, C., V. Robbe-Saule, and F. Norel.** 1996. Virulence and vaccine potential of *Salmonella typhimurium* mutants deficient in the expression of the RpoS (sigma S) regulon. Mol. Microbiol. **22:**149-60.

10. **DeLano, W. L.** 2002. Unraveling hot spots in binding interfaces: progress and challenges. Curr Opin Struct Biol. **12**:14-20.

11. **Dove, S. L., S. A. Darst, and A. Hochschild**. 2003. Region 4 of sigma as a target for transcription regulation. Mol Microbiol. **48**: 863-74.

12. **England, P., L. F. Westblade, G. Karimova, V. Robbe-Saule, F. Norel, and A. Kolb**. 2008. Binding of the unorthodox transcription activator, Crl, to the components of the transcription machinery. J Biol Chem. 283:33455-64.

13. **Ferenci, T**. 2005. Maintaining a healthy SPANC balance through regulatory and mutational adaptation. Mol Microbiol. **57**: 1-8.

14. **Gaal, T., M. J. Mandel, T. J. Silhavy, and R. L. Gourse**. 2006. Crl facilitates RNA polymerase holoenzyme formation. J. Bacteriol**. 188** : 7966-70.

15. **Geszvain, K., T. M. Gruber, R.A. Mooney, C. A. Gross, and R. Landick.** 2004. A hydrophobic patch on the flap-tip helix of *E. coli* RNA polymerase mediates σ^{70} region 4 function. J. Mol. Biol. **343**: 569-587.

16. **Grigorova, I. L., N. J. Phleger, V. K. Mutalik, and C. A. Gross.** 2006. Insights into transcriptional regulation and σ competition from an equilibrum model of RNA polymerase binding to DNA. Proc. Natl. Acad. Sci. USA **103**: 5332-5337.

17. **Gruber, T. M., and C. A. Gross.** 2003. Multiple sigma subunits and the partitioning of bacterial transcription space. Annu. Rev. Microbiol. **57**: 441-466.

18. **Ishihama, A.** 2000. Functional modulation of *Escherichia coli* RNA polymerase. Annu. Rev. Microbiol. **54:**499-518.

19. **Karimova G., J. Pidoux, A. Ullmann, and D. Ladant.** 1998. A bacterial two-hybrid system based on a reconstituted signal transduction pathway. Proc. Natl. Acad. Sci. USA. **95**: 5752-5756.

20. **Karimova, G., C. Robichon, and D. Ladant.** 2009. Characterization of YmgF, a 72-residue inner membrane protein that associates with the *Escherichia coli* cell division machinery. J. Bacteriol. **191**: 333-346.

21. **Klauck, E., A. Typas, and R. Hengge.** 2007. The σ^S subunit of RNA polymerase as a signal integrator and network master regulator in the general stress response in *Escherichia coli.* Sci. Prog. **90**: 103-127.

22. **Kowarz, L., C. Coynault, V. Robbe-Saule, and F. Norel.** 1994. The *Salmonella typhimurium katF* (*rpoS*) gene: cloning, nucleotide sequence, and regulation of *spvR* and *spvABCD* virulence plasmid genes. J. Bacteriol. **176:** 6852-60.

23. **Kuznedelov, K., L. Minakhin, A. Niedziela-Majka, S. L. Dove, D. Rogulja, B. E. Nickels, A. Hochschild, T. Heyduk, and K. Severinov**. 2002. A role for interaction of the RNA polymerase flap domain with the sigma subunit in promoter recognition. Science. **295**:855-7.

24. **Lane, W. J., and S. A. Darst.** 2006. The structural basis for promoter -35 element recognition by the group IV sigma factors. PLoS Biol. **9**:e269.

25. **Lederer, H., K. Mortensen., R. P. May, G. Baer, H. L. Cresp, D. Dersch, and H. Heumann**. 1991. Spatial arrangement of sigma-factor and core enzyme of *Escherichia coli* RNA polymerase. A neutron solution scattering study. .J. Mol. Biol. **219**:747-755

26. **Lonetto, M., M. Gribskov, and C. A. Gross.** 1992. The σ^{70} family: sequence conservation and evolutionary relationships. J. Bacteriol. **174**: 3843-3849.

27. **Miller, J. H.** 1972. Experiments in Molecular Genetics, Cold Spring Harbour, N. Y.

28. **Monteil V., A. Kolb, J. D'Alayer, P. Béguin, and F. Norel.** 2010. Identification of conserved amino acid residues of the *Salmonella* σ^S chaperone Crl involved in Crl-σ^S interactions. J. Bacteriol**. 192**: 1075-1087.

29. **Murakami, K.S., and S. A. Darst**. 2003. Bacterial RNA polymerase: the wholo story. Current Opin. Struct. Biol. **13**: 31-39.

30. **Nielsen, M., C. Lundegaard, O. Lund, and T.N. Petersen.** 2010. CPHmodels-3.0 - Remote homology modeling using structure guided sequence profiles. NAR web-issue, in Press

31. **Notley-McRobb, L., T. King, and T. Ferenci.** 2002. *rpoS* mutations and loss of general stress resistance in *Escherichia coli* populations as a consequence of conflict between competing stress responses. J. Bacteriol. **184**: 806-811

32. **Nyström T. 2004**. Growth versus maintenance: a trade-off dictated by RNA polymerase availability and sigma factor competition? Mol Microbiol. **54**: 855-62.

33. **Paget , M. S. B., and J. Helmann**. 2003. The σ^{70} family of sigma factors. Genome Biol. **4**: 203

34. **Patten, C. L., M. G. Kirchhof, M. R. Schertzberg, R.A. Morton, and H. E. Schellhorn.** 2004. Microarray analysis of RpoS-mediated gene expression in *Escherichia coli* K-12. Mol. Gen. Genomics**. 272** : 580-591

35. **Pratt, L. A., and T. J. Silhavy.** 1998. Crl stimulates RpoS activity during stationary phase. Mol. Microbiol. **29:** 1225-36.

36. **Robbe-Saule, V., G. Algorta, I. Rouilhac, and F. Norel.** 2003. Characterization of the RpoS status of clinical isolates of *Salmonella enterica*. Appl. Environ. Microbiol. **69**: 4352-4358.

37. **Robbe-Saule, V., I. Carreira, A. Kolb, and F. Norel**. 2008. Effect of growth temperature on Crl-dependent regulation of σ^S activity in *Salmonella enterica* serovar Typhimurium. J. Bacteriol. **190**: 4453-4459.

38. **Robbe-Saule V., C. Coynault, and F. Norel** 1995. The live oral typhoid vaccine Ty21a is a *rpoS* mutant and is susceptible to various environmental stresses. FEMS Microbiol. Lett. **126**: 171-176.

39. **Robbe-Saule, V., V., Jaumouille, M. C., Prevost, S., Guadagnini, C. Talhouarne, H. Mathout, A., Kolb A, and F. Norel.** 2006. Crl activates transcription initiation of RpoS-regulated genes involved in the multicellular behavior of *Salmonella enterica* serovar Typhimurium. J Bacteriol. **188** : 3983-94.

40. **Robbe-Saule, V., M. D., Lopes, A., Kolb, and F. Norel.** 2007. Physiological effects of Crl in *Salmonella* are modulated by σ^S level and promoter specificity. J. Bacteriol. **189**: 2976-2987.

41. **Sambrook, J., E. F. Fritsch and T. Maniatis.** 1989. Molecular cloning: a laboratory manual (2nd edn.), Cold Spring Harbor, N. Y.

42. **Schmieger, H.** 1972. Phage P22-mutants with increased or decreased transduction abilities. Mol. Gen. Genet. **119:** 75-88.

43. **Schwartz, E. C., A. Shekhtma, K. Dutta, M. R. Pratt , D. Cowburn, S. Darst, T. W. Muir.** 2008. A full-length group 1 bacterial sigma factor adopts a compact structure incompatible with DNA binding. Chem Biol. **15**:1091-103.

44. **Silhavy, T. J., M. L. Bernman and L. W. Ernqvist.** 1984. Experiments with Gene Fusions, Cold Spring Harbour, N. Y.

45. **Sternberg, N. L., and R. Maurer.** 1991. Bacteriophage-mediated generalized transduction in *Escherichia coli* and *Salmonella typhimurium*. Methods Enzymol. **204:** 18-43.

46. **Typas, A., C. Barembruch, A. Possling, and R. Hengge.** 2007. Stationary phase reorganisation of the *Escherichia coli* transcription machinery by Crl protein, a fine-tuner of σ^S activity and levels. The EMBO J. **26** : 1569-1578.

47. **Vassylyev, D. G., S-I. Sekine, O. Laptenko, J. Lee, M. N. Vassylyeva, S. Borukhov, and S. Yokoyama.** 2002. Crystal structure of a bacterial RNA polymerase holoenzyme at 2.6A resolution. Nature **417**: 712-719.

48. **Weber, H., T. Polen, J. Heuveling, V.F. Wendisch, and R. Hengge.** 2005. Genome-wide analysis of the general stress response network in *Escherichia coli*: σ^S-dependent genes, promoters, and sigma factor selectivity. J. Bacteriol. **187**: 1591-1603.

49. **Yuan, A. H., B. D. Gregory, J. S. Sharp, K. D. McCleary, S. L. Dove, and A. Hochschild.** 2008. Rsd family proteins make simultaneous interactions with regions 2 and 4 of the primary sigma factor. Mol. Microbiol. **70**: 1136-1151.

50. **Zambrano, M. M., and R. Kolter.** 1996. GASPing for life in stationary phase. Cell **86**:181-184.

51. **Zhou, Y., S. Gottesman, J. R. Hoskins, M. R. Maurizi, and S. Wickner**. 2001. The RssB reesponse regulator directly targets sigmaS for degradation by ClpXP. Genes Dev **15**: 627–637

Table 1: Bacterial strains and plasmids used in this study

Strain or plasmid	Characteristics	Source or reference[a]
Escherichia coli		
MC1061K	*araD139* Δ(*ara-leu*)*-767* Δ(*lacIPOZY*)*X74 rpsL galU galK rpoS::kan*	22
JM109	*recA*1 *supE*44 *endA*1 *hsdR*17 *gyrA*96 *relA*1 *thi* Δ(*lac-proAB*) F'(*traD*36 *proAB*$^+$ *lacI*^{q} *lacZ*ΔM15)	41
BTH101	F- *cya-99 araD139 galE15 galK16 rpsL1* (Str^R) *hsdR2 mcrA1 mcrB1*	D. Ladant
***Salmonella* serovar Typhi**		
5959	Wild-type, isolated from human blood	CNR[b]
5959*crl*	5959 Δ*crl*::Cm	
Ty19	Wild-type	CNR[b]
Ty19K	Ty19 Δ*rpoS*::Km	
Ty19*crl*	Ty19 Δ*crl*::Cm	
***Salmonella* serovar Typhimurium**		
ATCC14028	Wild-type	ATCC[c]
ATCC*rpoS*	ATCC14028 Δ*rpoS*::Cm	39
ATCC*crl*	ATCC14028 Δ*crl*::Cm	39
ATCCΔ*crl*	ATCC14028 Δ*crl*	39
2922K	ATCC14028 ΔSTM2922::Km	40

1	2922K*crl*	ATCC14028 ΔSTM2922::Km Δ*crl*::Cm	40
2	2922KΔ*crl*	ATCC14028 ΔSTM2922::Km Δ*crl*	
3	2922K*rpoS*	ATCC14028 ΔSTM2922::Km Δ*rpoS*::Cm	40
4	2922K$rpoS_{Ty19}$	ATCC14028 ΔSTM2922::Km $rpoS_{Ty19}$	
5	2922K$rpoS_{Ty19}$*crl*	2922K $rpoS_{Ty19}$ Δ*crl*::Cm	
6	2922K$rpoS_{Ty19}$Δ*crl*	2922K $rpoS_{Ty19}$ Δ*crl*	
7	2922K *katE-lacZ*	2922K Tn*5*B21-2.4	40
8	2922K*rpoS katE-lacZ*	2922K*rpoS* Tn*5*B21 –2.4	40
9	2922K*crl katE-lacZ*	2922K*crl* Tn*5*B21 –2.4	40
10	2922K$rpoS_{Ty19}$ *katE-lacZ*	2922K$rpoS_{Ty19}$ Tn*5*B21-2.4	
11	2922K$rpoS_{Ty19}$*crl katE-lacZ*	2922K $rpoS_{Ty19}$ Δ*crl*::Cm Tn*5*B21-2.4	
12			
13	**Plasmids**		
14	pACYC184	cloning vector, Cm^R, Tet^R	8
15	pUCK3Km	pUC19 with *S.* Typhimurium Δ*rpoS* ::Km, Cb^R Km^R	22
16	pUC4K	source of Km resistance cartridge	Pharmacia
17	pAC$rpoS_{Ty19}$	pACYC184 with a 6 kb *Bgl*II fragment	
18		carrying $rpoS_{Ty19}$, Cm^R	
19	pUC$rpoS_{Ty19}$	pUC19 with a 3.5 kb *Hind*III-*Sca*I fragment	
20		carrying $rpoS_{Ty19}$, Cb^R	
21	pUC$rpoS_{Ty19}$K	pUC$rpoS_{Ty19}$ with STY3047::Km, Cb^R Km^R	
22	pQE30	vector for expression of His-tagged proteins, Cb^R	Qiagen
23	pQE30*rpoS*	pQE30::*rpoS* expresses a His_6-σ^S protein, Cb^R	28
24	pQE30$rpoS_{Ty19}$	pQE30::*rpoS* expresses a His_6-$\sigma^S{}_{Ty19}$ protein, Cb^R	
25	pKT25	BACTH vector designed to express a given	20

		polypeptide fused in frame at its N-terminal end with	
		T25 fragment, p15 ori, Km^R	
pUT18		BACTH vector designed to express a given	20
		polypeptide fused in frame at its C-terminal end with	
		T18 fragment, ColE1 ori, Ap^R	
pUTCrl		pUT18 expressing Crl-T18	28
pKTRpoS		pKT25 expressing T25-σ^S	28
$pKTRpoS_{Ty19}$		pKT25 expressing T25-σ^S_{Ty19}	
$pKTRpoS_{\Delta 1-71}$		pKT25 expressing T25-σ^S_{72-330}	28
$pKTRpoS_{90-330}$		pKT25 expressing T25-σ^S_{90-330}	
$pKTRpoS_{90-330Ty19}$		pKT25 expressing T25-$\sigma^S_{90-330Ty19}$	
$pKTRpoS_{169-330}$		pKT25 expressing T25-$\sigma^S_{169-330}$	
$pKTRpoS_{238-330}$		pKT25 expressing T25-$\sigma^S_{238-330}$	
$pKTRpoS_{238-330Ty19}$		pKT25 expressing T25-$\sigma^S_{238-330Ty19}$	
$pKTRpoS_{1-254}$		pKT25 expressing T25-σ^S_{1-254}	
$pKTRpoS_{72-254}$		pKT25 expressing T25-σ^S_{72-254}	
$pKTRpoS_{1-167}$		pKT25 expressing T25-σ^S_{1-167}	
$pKTRpoS_{56-167}$		pKT25 expressing T25-σ^S_{56-167}	
$pKTRpoS_{72-167}$		pKT25 expressing T25-σ^S_{72-167}	

[a] This study, unless otherwise noted.

[b] National Reference Center for *Salmonella* (Institut Pasteur, Paris)

[c] American Type Culture Collection

LEGENDS TO FIGURES

FIGURE 1. Detection of σ^S and σ^S_{Ty19} in *S.* Typhi (STY) and *S*. Typhimurium (STM). Overnight LB cultures at 37°C were analysed by western blotting with anti-σ^S antibodies. 5 µg of total protein was loaded in each slot. 1: 5959, 2: Ty19, 3: Ty19K, 4: 2922K, 5: 2922K*crl*, 6: 2922K*rpoS*, 7: 2922K*rpoS*$_{Ty19}$, 8: 2922K*rpoS*$_{Ty19}$*crl*.

FIGURE 2. *In vivo* characterization of the *rpoS*$_{Ty19}$ mutant allele. ABC) Resistance to hydrogen peroxide of *Salmonella* strains carrying wild-type or *rpoS*$_{Ty19}$ mutant alleles. A) *S.* Typhi strains 1: 5959, 2: 5959*crl*, 3: Ty19, 4: Ty19*crl*, 5: Ty19K. B) *S.* Typhi strains 5959 (WT), Ty19, Ty19*crl*, Ty19K. C) *S*. Typhimurium strains 2922K (WT), 2922KΔ*crl*, 2922K*rpoS*$_{Ty19}$, 2922K*rpoS*$_{Ty19}$Δ*crl*, 2922K*rpoS*. Cells were grown to stationary phase in LB at 37°C, washed, resuspended in PBS to an OD_{600} of 1 (A) and 0.1 (BC) and H_2O_2 15 mM was added. Representative experiments are shown in BC. Similar results were obtained in repeat experiments. D) Expression of a *katE-lacZ* gene fusion in *S.* Typhimurium carrying the wild-type *rpoS* and mutant *rpoS*$_{Ty19}$ alleles. 1: 2922K*katE-lacZ,* 2: 2922K*rpoS katE-lacZ*, 3: 2922K*crl katE-lacZ*, 4: 2922K*rpoS*$_{Ty19}$ *katE-lacZ*, 5: 2922K*rpoS*$_{Ty19}$*crl katE-lacZ*. β-galactosidase activity was measured in overnight LB cultures at 37°C according to the method of Miller (27).

FIGURE 3. *In vitro* characterization of the *rpoS*$_{Ty19}$ mutant allele. A). Single round run-off transcripts of *katE* (lanes 1-4), *katN* (lanes 5-8) and *poxB* (lanes 9-12) promoters. RNA polymerases reconstituted with His$_6$-σ^S_{Ty19} (lanes 1-2, 5-6 and 9-10) or His$_6$-σ^S_{WT} (lanes 3-4, 7-8 and 11-12) in the absence (lanes 1, 3, 5, 7, 9 and 11) or presence of Crl (lanes 2, 4, 6, 8, 10 and 12) were incubated with plasmid templates for 12 min at 30°C before addition of a

mixture of heparin and XTPs as described in Materials and Methods. The ^{32}P–labelled transcripts were analysed on a 7 % sequencing gel and the band intensities quantified as indicated below each lane. B). Real-time SPR experiments showing the effect of Crl (5 μM) on the binding of His_6-σ^S_{Ty19} (left; 625 nM) or His_6-σ^S_{WT} (right; 625 nM) to the immobilized RNAP core. The sensorgrams shown in blue and cyan correspond to the binding of σ^S in the absence of Crl, and those in red and magenta to that in the presence of Crl. No E-binding of His_6-σ^S_{Ty19} can be detected in the absence of Crl.

FIGURE 4. Crl binds to σ^S domain 2. A) Model of the σ^S structure. The structural domains σ_2 (residues 53–163), σ_3 (residues 164-216), linker (residues 217-244) and σ_4 (residues 245-314) are represented in light green, yellow, orange and blue, respectively. The G282 is represented in red. B) BACTH analysis of Crl interactions with σ^S, σ^S_{Ty19} and truncated σ^S proteins. A schematic representation of the four regions of the σ^S protein showing highly conserved amino acid sequence with the σ^{70} family members (7, 26) is shown at the top of the figure. The efficiencies of functional complementation between the indicated hybrid proteins were quantified by measuring β-galactosidase activities in *E. coli* BTH101 cells harboring the corresponding plasmids as described in Material and Methods. β-galactosidase activity was measured according to the method of Miller (27).

FIGURE 5. Position of the G282V substitution that affects the interaction of σ^S_{Ty19} with the RNAP core enzyme. A) Structure of the modelled σ^S positioned in the *T. thermophilus* enzyme core. The αI, αII, β, β' and ω subunits are represented in pale yellow, wheat, dark red, pink and pale orange, respectively. The region corresponding to the β-flap is coloured in

orange, and the region corresponding to the β' zinc finger in cyan. B) Close-up view of the interaction between the core enzyme and σ_4. A valine is shown at position 282 of the σ^S.

FIGURE 6. Survival and competitive fitness of *Salmonella* strains during stationary phase. (A) Survival in stationary-phase cultures in LB medium at 37°C. Cells from overnight LB cultures of *S.* Typhimurium (a) and S. Typhi (b) strains indicated were washed, resuspended in PBS to an OD_{600} of 1.0, diluted in fresh LB medium and incubated at 37°C with shaking. Aliquots of bacteria were removed at timed intervals and numbers of viable cells were determined on LB plates. One hundred percent survival corresponds to the number of cells in cultures grown overnight (day 1). Representative experiments are shown. Similar results were obtained in repeat experiments. (B) Competition assays between *S.* Typhimurium (abcdefg) and *S.* Typhi (h) strains. Overnight LB cultures were washed and resuspended in PBS to an OD_{600} of 1.0. In each of the eight experiments, the two strains indicated were mixed in equal cell numbers in fresh LB medium to give a total of about 3000 cells ml^{-1} (time zero) and the mixtures were incubated at 37°C with shaking. Aliquots of bacteria were removed at timed intervals and numbers of viable cells of each strain were determined. Numbers of cells of each strain are reported as a percentage of the total number of viable cells in the culture.

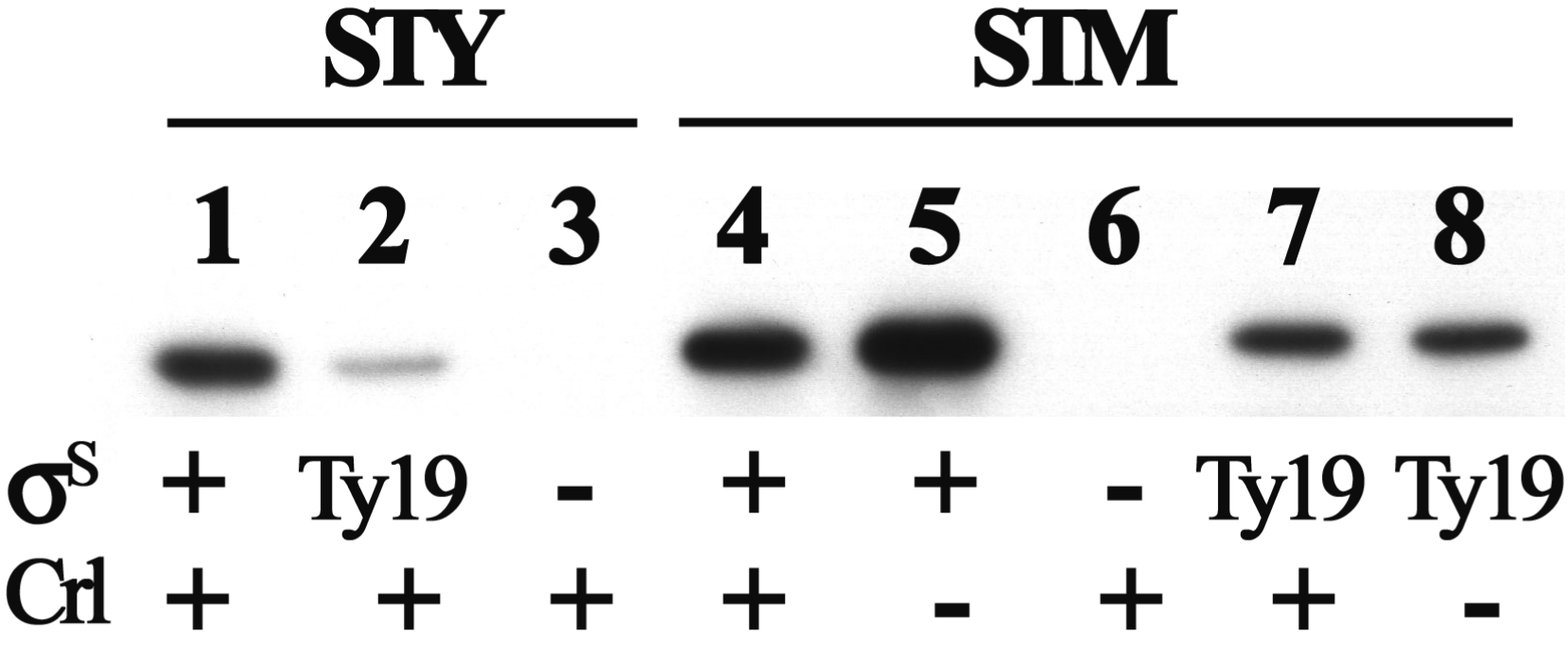
STY
STM
1 2 3 4 5 6 7 8
σS + Ty19 - + + - Ty19 Ty19
Crl + + + + - + + -

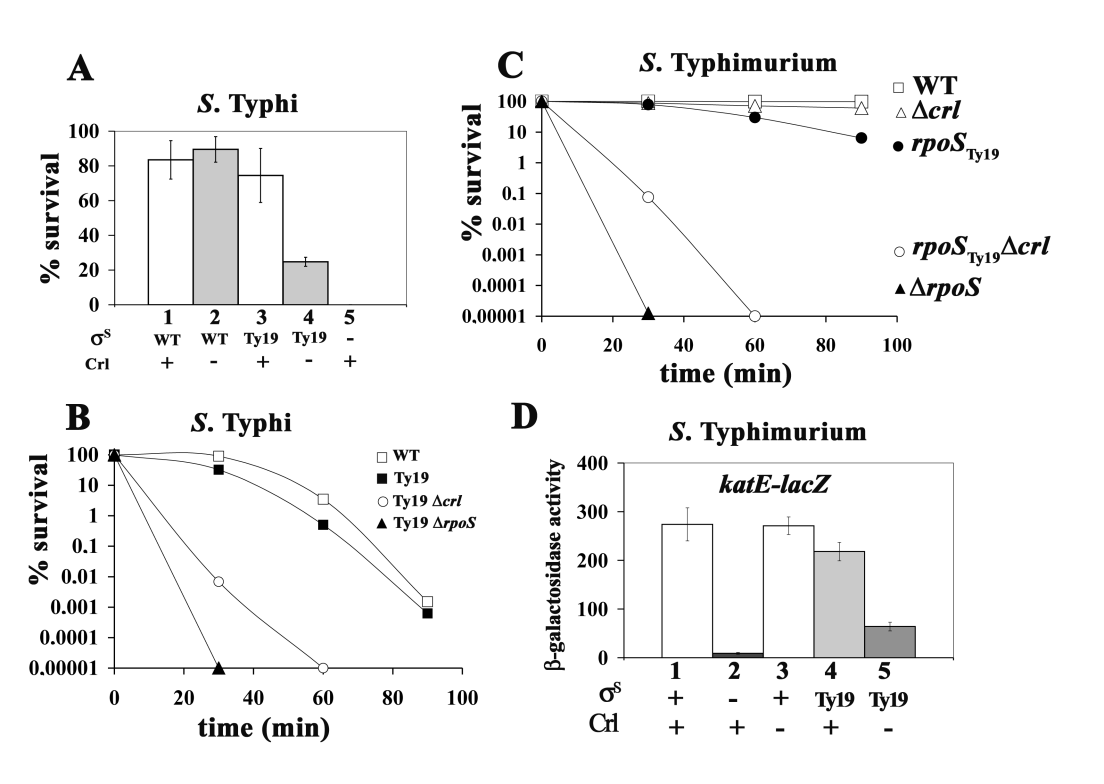
A
S. Typhi
% survival
100
80
60
40
20
0
1 2 3 4 5
σS WT WT Ty19 Ty19 -
Crl + - + - +
B
S. Typhi
% survival
100
10
1
0.1
0.01
0.001
0.0001
0.00001
0 20 40 60 80 100
time (min)
WT
Ty19
Ty19 Δcrl
Ty19 ΔrpoS
C
S. Typhimurium
% survival
100
10
1
0.1
0.01
0.001
0.0001
0.00001
0 20 40 60 80 100
time (min)
WT
Δcrl
rpoSTy19
rpoSTy19Δcrl
ΔrpoS
D
S. Typhimurium
katE-lacZ
β-galactosidase activity
400
300
200
100
0
1 2 3 4 5
σS + - + Ty19 Ty19
Crl + + - + -

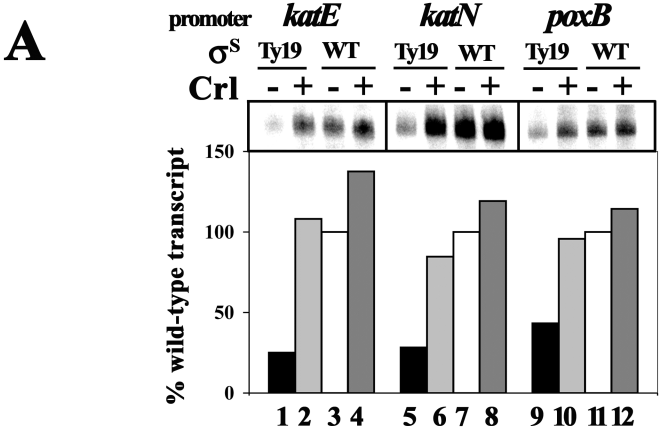
A
promoter
katE
katN
poxB
σS
Ty19
WT
Ty19
WT
Ty19
WT
Crl
- + - + - + - + - + - +
% wild-type transcript
150
100
50
0
1 2 3 4 5 6 7 8 9 10 11 12

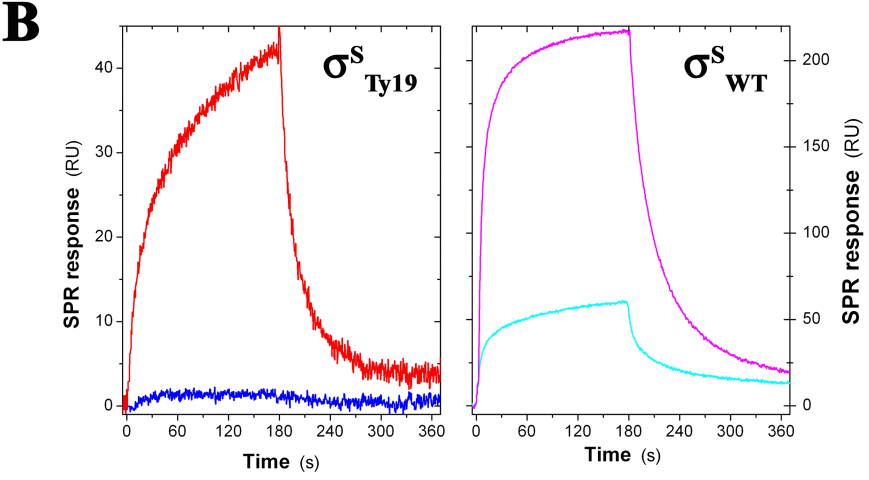
B
σS Ty19
σS WT
SPR response (RU)
SPR response (RU)
Time (s)
Time (s)
0 60 120 180 240 300 360
0 10 20 30 40
0 50 100 150 200

A

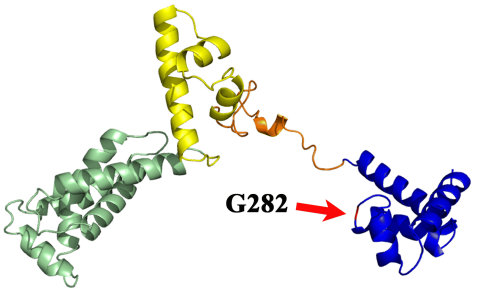

B

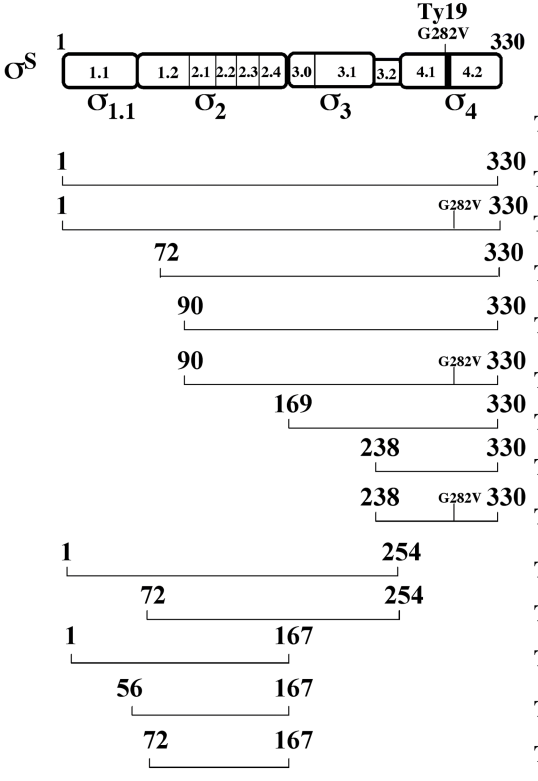

	+ Crl-T18 β-galactosidase activity
T25	59 ± 2
T25-σ^S	273 ± 36
T25-σ$^S_{Ty19}$	1554 ± 134
T25-σ$^S_{72-330}$	2236 ± 265
T25-σ$^S_{90-330}$	51 ± 4
T25-σ$^S_{90-330\ Ty19}$	52 ± 4
T25-σ$^S_{169-330}$	55 ± 5
T25-σ$^S_{238-330}$	62 ± 12
T25-σ$^S_{238-330\ Ty19}$	59 ± 5
T25-σ$^S_{1-254}$	629 ± 24
T25-σ$^S_{72-254}$	1009 ± 84
T25-σ$^S_{1-167}$	2020 ± 185
T25-σ$^S_{56-167}$	1268 ± 132
T25-σ$^S_{72-167}$	610 ± 57

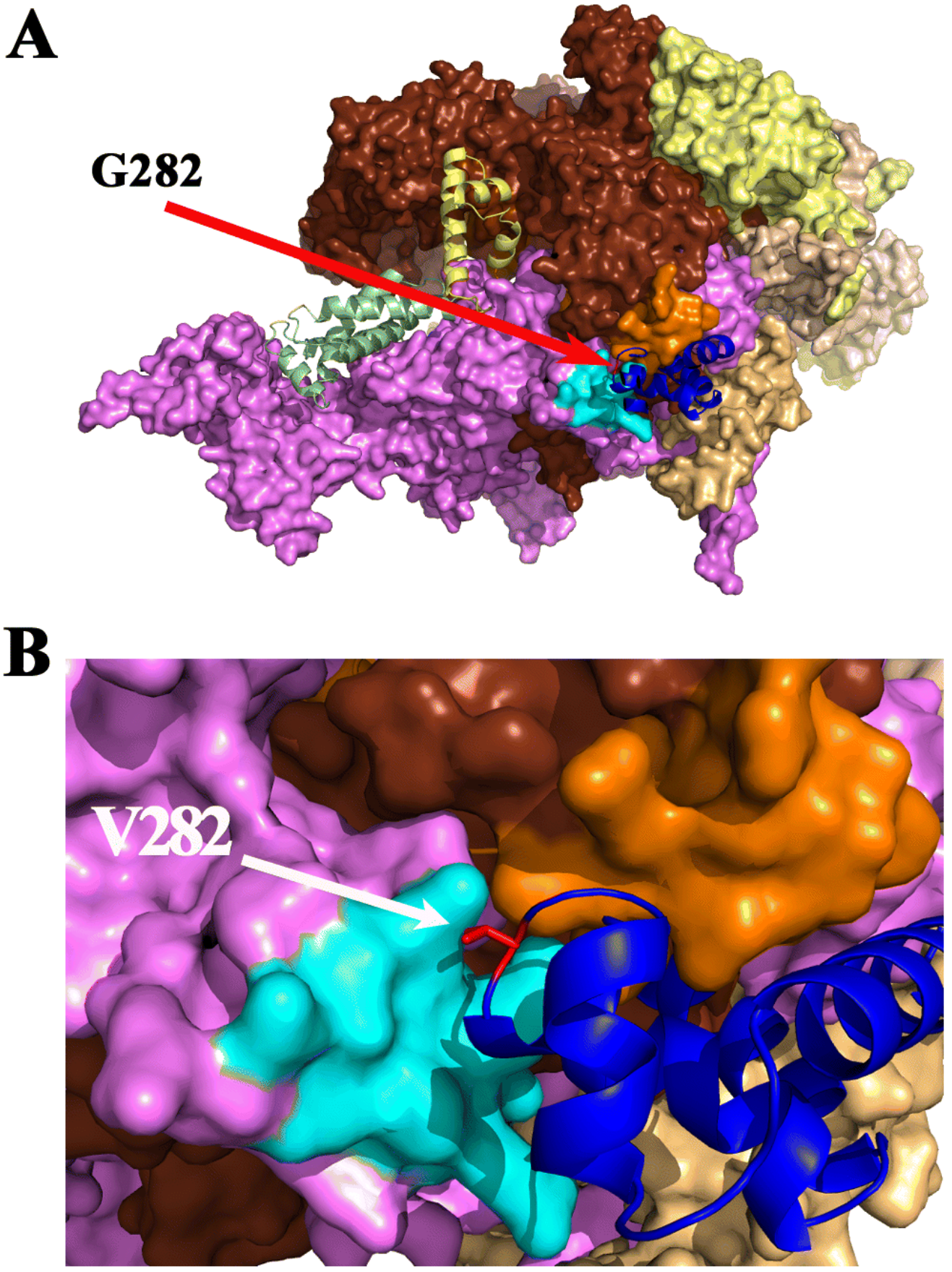
A
G282
B
V282

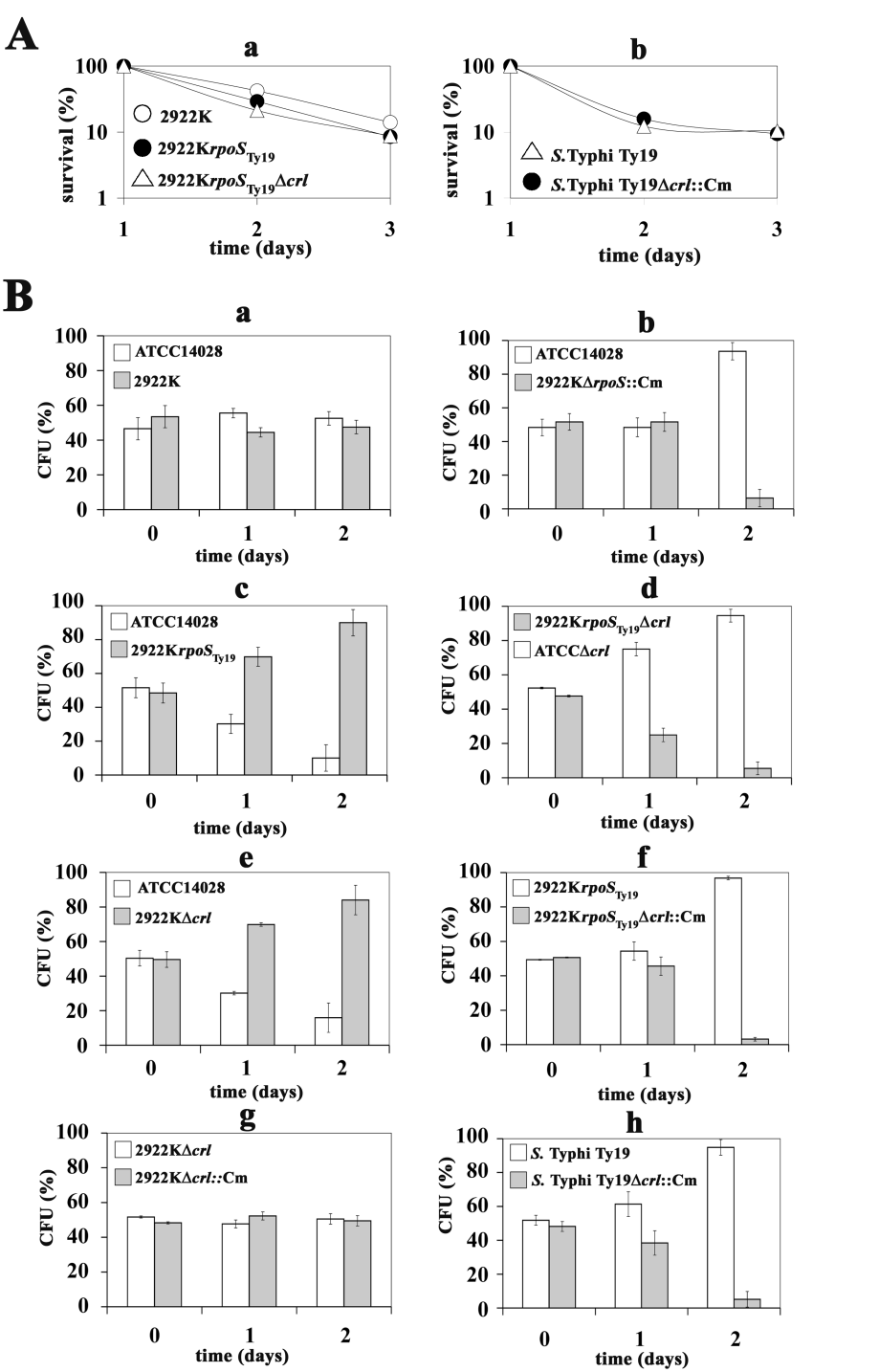
A
a
100
10
1
survival (%)
2922K
2922K*rpoS*Ty19
2922K*rpoS*Ty19Δ*crl*
1
2
3
time (days)
b
100
10
1
survival (%)
*S.*Typhi Ty19
*S.*Typhi Ty19Δ*crl*::Cm
1
2
3
time (days)
B
a
ATCC14028
2922K
CFU (%)
0
20
40
60
80
100
0
1
2
time (days)
b
ATCC14028
2922KΔ*rpoS*::Cm
CFU (%)
time (days)
c
ATCC14028
2922K*rpoS*Ty19
CFU (%)
time (days)
d
2922K*rpoS*Ty19Δ*crl*
ATCCΔ*crl*
CFU (%)
time (days)
e
ATCC14028
2922KΔ*crl*
CFU (%)
time (days)
f
2922K*rpoS*Ty19
2922K*rpoS*Ty19Δ*crl*::Cm
CFU (%)
time (days)
g
2922KΔ*crl*
2922KΔ*crl*::Cm
CFU (%)
time (days)
h
S. Typhi Ty19
S. Typhi Ty19Δ*crl*::Cm
CFU (%)
time (days)